

A New Allenyl Bonding Mode in Binuclear Complexes: Characterization and Molecular Structures of $M_2(CO)_6(\mu\text{-PPh}_2)(\mu\text{-}\eta^1\text{:}\eta^2_{\beta,\gamma}\text{-C(Ph)=C=CH}_2)$ ($M = \text{Ru, Os}$)

Neil Carleton, John F. Corrigan, Simon Doherty, Robin Pixner, Yan Sun, Nicholas J. Taylor, and Arthur J. Carty*

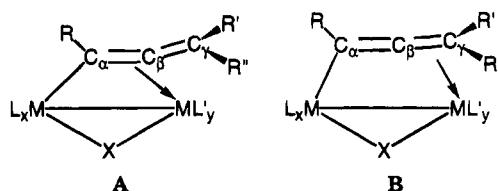
Guelph-Waterloo Centre for Graduate Work in Chemistry, Waterloo Campus, Department of Chemistry, University of Waterloo, Waterloo, Ontario N2L 3G1, Canada

Received March 25, 1994[®]

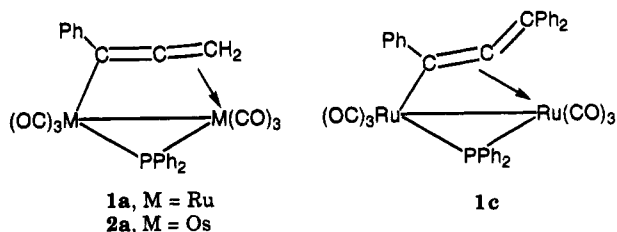
Summary: The binuclear allenyl complexes $M_2(CO)_6(\mu\text{-PPh}_2)(\mu\text{-}\eta^1\text{:}\eta^2_{\beta,\gamma}\text{-C(Ph)=C=CH}_2)$ (**1a**, $M = \text{Ru}$; **2a**, $M = \text{Os}$), obtained from the $\mu\text{-}\eta^1\text{:}\eta^2$ -acetylides $M_2(CO)_6(\mu\text{-PPh}_2)(\mu\text{-}\eta^1\text{:}\eta^2\text{-C}\equiv\text{CPh})$ via reaction with diazomethane, have unprecedented structures in which C_α is σ -bonded to one metal site while the $C_\beta\text{-}C_\gamma$ double bond is coordinated to the second metal. Previously only $\mu\text{-}\eta^1\text{:}\eta^2_{\alpha,\beta}$ and $\mu\text{-}\eta^2_{\alpha,\beta}\text{:}\eta^3_{\alpha,\beta,\gamma}$ bonding modes were known for the allenyl ligand on dinuclear centers. Reaction of **1a** with $\text{Ph}_2\text{PCH}_2\text{PPh}_2$ affords $\text{Ru}_2(\text{CO})_4(\mu\text{-DPPM})[\mu\text{-}\eta^2, \eta^3\text{-P(Ph}_2\text{)C(O)C(Ph)CCH}_2]$ (**6**), containing a novel allenyl-carbonyl-phosphido ligand.

The allenyl fragment -C(H)=C=CH_2 is a cumulated C_3 hydrocarbyl ligand, for which an extensive organometallic chemistry is beginning to develop.¹ In addition to η^1 and η^3 coordination in monometallic compounds,² four bonding modes have been established in polynuclear systems where the allenyl group occupies a bridging position. For binuclear complexes $\mu\text{-}\eta^2\text{:}\eta^3$ and $\mu\text{-}\eta^1\text{:}\eta^2$ bonding is well established,³ with the π -bound metal in the latter case attached to the $C_\alpha\text{-}C_\beta$ double bond. For tri- and tetranuclear clusters the more common $\mu_3\text{-}\eta^1\text{:}\eta^2\text{:}\eta^2$ ⁴ and less frequent $\mu_4\text{-}\eta^1\text{:}\eta^2\text{:}\eta^2\text{:}\eta^2$ ⁵ bridging modes are known. We now report a previously unknown coordination mode for an allenyl group in the binuclear systems in which the near-linearity of the cumulated, metalated allene is retained and demonstrate the existence of both $\mu\text{-}\eta^1\text{:}\eta^2_{\alpha,\beta}$ (**A**) and $\mu\text{-}\eta^1\text{:}\eta^2_{\beta,\gamma}$

(**B**) bonding⁶ in complexes of the type $M_2(CO)_6(\mu\text{-PPh}_2)[\mu\text{-}\eta^1\text{:}\eta^2\text{-C(Ph)=C=CR}_2]$ ($M = \text{Ru}$ (**1**), Os (**2**)).



The series of complexes **1** ($M = \text{Ru}$, $R = \text{H}$ (**1a**) Me (**1b**) Ph (**1c**)) is accessible via carbon-carbon coupling reactions between diazoalkanes and acetylides $\text{Ru}_2(\text{CO})_6(\mu\text{-PPh}_2)(\mu\text{-}\eta^1\text{:}\eta^2\text{-C}\equiv\text{CPh})$.⁷ The complex **1c** has structure **A**, in which the allenyl ligand is $\mu\text{-}\eta^1\text{:}\eta^2_{\alpha,\beta}$ -bound. Other heterobinuclear allenyl complexes have also been shown to have similar $\mu\text{-}\eta^1\text{:}\eta^2_{\alpha,\beta}$ coordination.^{3c,8} An isomeric, as yet undocumented structure for complexes of formula **1** and related homo- or heterometallic allenyls is **B**, in which the outer $C_\beta\text{-}C_\gamma$ double bond of the allenyl group is coordinated.



Chemically **1a** is extremely reactive toward nucleophiles, forming saturated and unsaturated metalocycles via exclusive nucleophilic attack at C_β .^{9a} Other allenyls, including some η^1 -bound ligands, also show a propensity for attack at C_β .⁹ In contrast, some heterobimetallic $\mu\text{-}\eta^1\text{:}\eta^2_{\alpha,\beta}$ allenyls appear to be unreactive toward nucleophiles at the hydrocarbyl sites.¹⁰ The distinctive

(6) For convenience we use the nomenclature $\mu\text{-}\eta^1\text{:}\eta^2_{\alpha,\beta}$ to designate coordination of the $C_\alpha\text{-}C_\beta$ double bond to the second metal site. Thus, $\mu\text{-}\eta^1\text{:}\eta^2_{\beta,\gamma}$ indicates attachment of the $C_\beta\text{-}C_\gamma$ double bond to the π -bound metal.

(7) Cherkas, A. A.; Randall, S.; MacLaughlin, S. A.; Mott, G. N.; Taylor, N. J.; Carty, A. J. *Organometallics* **1988**, *7*, 969.

(8) (a) Young, G. H.; Wojcicki, A. J. *Am. Chem. Soc.* **1989**, *111*, 6890. (b) Young, G. H.; Raphael, M. V.; Wojcicki, A.; Calligaris, M.; Narden, G.; Bresciani-Pahor, N. *Organometallics* **1991**, *10*, 1934.

(9) (a) Breckenridge, S. M.; Taylor, N. J.; Carty, A. J. *Organometallics* **1991**, *10*, 837. (b) Chen, J. T.; Huang, T.-M.; Cheng, M.-C.; Lin, Y.-C.; Wang, Y. *Organometallics* **1992**, *11*, 1761. (c) Huang, T.-M.; Chen, J. T.; Lee, G.-H.; Wang, Y. *J. Am. Chem. Soc.* **1993**, *115*, 1170. (d) Blosser, P. W.; Schimplf, D. G.; Gallucci, J. C.; Wojcicki, A. *Organometallics* **1993**, *12*, 3864.

(10) Wojcicki, A.; Schuchart, C. E. *Coord. Chem. Rev.* **1990**, *105*, 35.

[®] Abstract published in *Advance ACS Abstracts*, October 15, 1994.

(1) (a) Doherty, S.; Corrigan, J. F.; Carty, A. J.; Sappa, E. *Adv. Organomet. Chem.*, in press. (b) Wojcicki, A. *J. Cluster Sci.* **1993**, *4*, 59. (c) Wojcicki, A. *New J. Chem.* **1994**, *18*, 61.

(2) For recent references see: (a) Stang, P. J.; Critell, C. M.; Arif, A. M. *Organometallics* **1993**, *12*, 4799. (b) Blosser, P. W.; Gallucci, J. C.; Wojcicki, A. *J. Am. Chem. Soc.* **1993**, *115*, 2994. (c) Blosser, P. W.; Schimplf, D. G.; Gallucci, J. C.; Wojcicki, A. *Organometallics* **1993**, *12*, 1993. (d) Wouters, J. M. A.; Klein, R. A.; Elsevier, C. E.; Zoutberg, M. C.; Stam, C. H. *Organometallics* **1993**, *12*, 3864. (e) Casey, C. P.; Yi, C. S. *J. Am. Chem. Soc.* **1992**, *114*, 6597. (f) Pu, J.; Peng, T.-S.; Arif, A. M.; Gladysz, J. A. *Organometallics* **1992**, *11*, 3232.

(3) (a) Young, G. H.; Raphael, M. V.; Wojcicki, A.; Calligaris, M.; Nardin, G.; Bresciani-Pahor, N. *Organometallics* **1991**, *10*, 1934. (b) Seyferth, D.; Womack, G. B.; Archer, C. M.; Dewan, J. C. *Organometallics* **1989**, *8*, 430. (c) Dickson, R. S.; Jenkins, S. M.; Skelton, B. W.; White, A. H. *Polyhedron* **1988**, *7*, 859. (d) Meyer, A.; McCabe, D. J.; Curtis, M. D. *Organometallics* **1987**, *6*, 1491. (e) Casey, C. P.; Woo, L. K.; Fagen, P. J.; Palermo, R. E.; Adams, B. R. *Organometallics* **1987**, *6*, 447. (f) Nucciarone, D.; Taylor, N. J.; Carty, A. J. *Organometallics* **1986**, *5*, 1179.

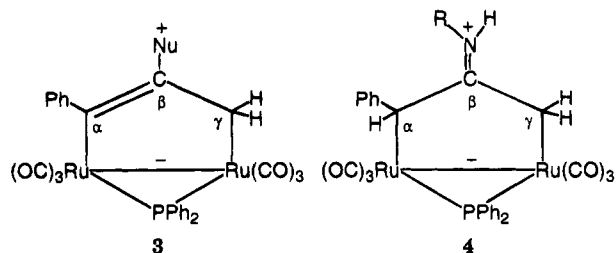
(4) (a) Nucciarone, D.; MacLaughlin, S. A.; Taylor, N. J.; Carty, A. J. *Organometallics* **1988**, *7*, 106. (b) Suades, J.; Dahan, F.; Mathieu, R. *Organometallics* **1988**, *7*, 47. (c) Aime, S.; Osella, D.; Deeming, A. J.; Arce, A. J.; Hurthouse, M. B.; Dawes, H. M. *J. Chem. Soc., Dalton Trans.* **1986**, 1459.

(5) Attali, S.; Dahan, F.; Mathieu, R. *Organometallics* **1986**, *5*, 1376.

reactivity of **1a** together with some unusual NMR features prompted us to synthesize the corresponding diosmium complex **2a** and undertake a detailed study of structure–reactivity relationships for **1a**, its diphenyl derivative **1c**, and **2a**. In this communication we describe the unprecedented structures of **1a** and **2a**, an EHMO analysis modeling their chemical reactivity patterns, and further studies indicating novel reaction chemistry.

The preparative route to **1a** and **2a** involves treatment of $\text{Ru}_2(\text{CO})_6(\mu\text{-PPh}_2)(\mu\text{-}\eta^1\text{:}\eta^2\text{-C}\equiv\text{CPh})$ and $\text{Os}_2(\text{CO})_6(\mu\text{-PPh}_2)(\mu\text{-}\eta^1\text{:}\eta^2\text{-C}\equiv\text{CPh})^7$ with N_2CH_2 at 295 K, giving high yields of **1a** and **2a**, respectively (Scheme 1). The $^{13}\text{C}\{^1\text{H}\}$ NMR spectrum of **1a**¹¹ revealed, in contrast to that of **1c**, a static structure on the NMR time scale indicative of an unusual bonding arrangement of the hydrocarbyl ligand. The chemical shifts in binuclear allenyl complexes^{3a,8,12} generally move to higher field in the order $\delta(\text{C}_\beta) > \delta(\text{C}_\alpha) > \delta(\text{C}_\gamma)$. For **1a**¹¹ (R = H) and **2a**,¹³ however, a different trend was observed with $\delta(\text{C}_\alpha)$ (**1a**, 141.1; **2a**, 142.1 ppm) $>$ $\delta(\text{C}_\beta)$ (**1a**, 99.2; **2a** 88.3 ppm) \gg $\delta(\text{C}_\gamma)$ (**1a**, 1.0; **2a**, -3.3 ppm).¹⁴ Indeed, the chemical shifts and the $^1J_{\text{CH}}$ values of C_γ (**1a**, $^1J_{\text{CH}} = 169$ Hz; **2a**, $^1J_{\text{CH}} = 170$ Hz) lie in the range observed for the corresponding carbon atom in the dimetallacyclopentene (**3**) and dimetalloacyclopentane (**4**) derivatives.^{9a} Single-crystal X-ray analyses of **1a**¹⁵ and **2a**¹⁶ were carried out to fully elucidate the structural characteristics of the bridging hydrocarbyl ligand.

The molecular structure of **1a** (Figure 1) shows that addition of the H_2C moiety has occurred at C_α of the acetylide precursor, affording an allenyl moiety bound



to two ruthenium atoms ($\text{Ru}(1)\text{--Ru}(2) = 2.860(1)$ Å) also bridged symmetrically by a phosphido group ($\text{Ru}(1)\text{--P}(1) = 2.331(1)$ Å; $\text{Ru}(2)\text{--P}(1) = 2.348(1)$ Å). Of particular interest is the allenyl ligand, which is σ -bonded via $\text{C}(7)$ to $\text{Ru}(1)$ ($2.132(3)$ Å) and π -bonded to $\text{Ru}(2)$ through $\text{C}(8)$ and $\text{C}(9)$ ($\text{Ru}(2)\text{--C}(8) = 2.370(3)$ Å; $\text{Ru}(2)\text{--C}(9) = 2.335(3)$ Å). The bond lengths $\text{C}(7)\text{--C}(8)$ ($1.296(4)$ Å) and $\text{C}(8)\text{--C}(9)$ ($1.355(5)$ Å) are significantly different and reflect this bonding arrangement. This is the first instance in which an allenyl fragment has been found to have the $\text{C}_\beta\text{--C}_\gamma$ double bond uniquely coordinated in a π fashion to a second metal atom. Wojcicki and co-workers have reported the synthesis of the heterobimetallic ketoallenyl complex $[\text{RuFe}(\text{CO})_4\text{Cp}(\mu\text{-}\eta^2\text{:}\eta^3\text{-C}(\text{O})\text{C}(\text{Ph})\text{C}=\text{CH}_2)]$ (**5**).^{10,17} The presence of an inserted carbonyl reduces the strain otherwise present in the allenyl ligand ($\text{C--C--C} \approx 145^\circ$), allowing coordination of the internal $\text{C}=\text{C}$ ($\text{C}_\alpha\text{--C}_\beta$) bond to the iron center and the external $\text{C}_\beta\text{--C}_\gamma$ bond to the ruthenium atom. In the related complex $\text{Ru}_2(\text{CO})_6(\mu\text{-PPh}_2)[\mu\text{-C}(\text{Ph})=\text{C}=\text{CPh}_2]$ (**1c**)^{3f} the allenyl ligand is σ -bonded via C_α but π -bonded through C_α and C_β ($\text{Ru}(1)\text{--C}(7) = 2.102(7)$ Å; $\text{Ru}(2)\text{--C}(7) = 2.374(6)$ Å; $\text{Ru}(2)\text{--C}(8) = 2.173(7)$ Å; $\text{C}(7)\text{--C}(8) = 1.382(11)$ Å; $\text{C}(8)\text{--C}(9) = 1.350(12)$ Å). In **1a** the hydrocarbyl ligand is less sterically demanding than in **1c**, and this may account for the adoption of an unprecedented $\mu\text{-}\eta^1\text{:}\eta^2_{\beta,\gamma}$ arrangement. The angle $\text{C}(7)\text{--C}(8)\text{--C}(9)$ ($172.3(3)^\circ$) in **1a** reflects the near-linearity of the ligand, and indeed, the resemblance to a metalated allene is much greater than in **1c** ($\text{C}(7)\text{--C}(8)\text{--C}(9) = 144.0(4)^\circ$). Crystals of **1a** and **2a** are isomorphous and isostructural (Figure 1), with the Os--C and C--C distances in **2a** essentially unchanged from those in **1a** ($\text{Os}(1)\text{--C}(7) = 2.15(1)$ Å; $\text{Os}(2)\text{--C}(8) = 2.35(1)$ Å; $\text{Os}(2)\text{--C}(9) = 2.34(1)$ Å; $\text{C}(7)\text{--C}(8) = 1.27(2)$ Å; $\text{C}(8)\text{--C}(9) = 1.35(2)$ Å). We have performed EHMO¹⁸ studies on the model complex $\text{Ru}_2(\text{CO})_6(\mu\text{-PPh}_2)(\mu\text{-}\eta^1\text{:}\eta^2_{\beta,\gamma}\text{-HCCCH}_2)$ to evaluate the contributions of the allenyl carbon atoms to the LUMO and SLUMO, since the selectivity toward nucleophilic attack might presumably be defined by the nature of these orbitals.

(11) Selected data for **1a**: IR (C_6H_{12}) $\nu(\text{CO})$ 2075 s, 2044 s, 2011 s, 1995 m, 1904 w cm^{-1} ; $^{31}\text{P}\{^1\text{H}\}$ NMR (CDCl_3) δ 138.3 ppm; $^{13}\text{C}\{^1\text{H}\}$ NMR (CD_2Cl_2) δ 199.8 (d, $^2J_{\text{PC}} = 12.1$ Hz, CO), 198.2 (s, CO), 198.1 (d, $^2J_{\text{PC}} \approx 9$ Hz, CO), 196.9 (d, $^2J_{\text{PC}} = 31.7$ Hz, CO), 196.6 (d, $^2J_{\text{PC}} = 12.1$ Hz, CO), 195.5 (d, $^2J_{\text{PC}} = 28.7$ Hz, CO), 141.1 (s, C_α), 140.2 (d, $^1J_{\text{PC}} = 29.0$ Hz, C_{ipso}), 139.2 (d, $^2J_{\text{PC}} = 5.5$ Hz, C_{ipso}), 133.6–127.1 (mult, C_{phenyl}), 99.2 (s, C_β), 1.0 (s, C_γ) ppm; ^1H NMR (CD_2Cl_2) δ 7.68–7.00 (mult, 15H, H_{phenyl}), 2.11 (d, $^2J_{\text{HH}} = 6.3$ Hz, 1H, $=\text{CH}_a\text{H}_b$), 1.46 (dd, $^2J_{\text{HH}} = 6.3$ Hz, $^3J_{\text{PH}} = 2.6$ Hz, 1H, $=\text{CH}_a\text{H}_b$) ppm. Anal. Calcd for $\text{C}_{27}\text{H}_{17}\text{O}_6\text{PRu}_2\text{CH}_2\text{Cl}_2$: C, 44.52; H, 2.53. Found: C, 44.77; H, 2.47.

(12) Cherkas, A. A.; Breckenridge, S. M.; Carty, A. J. *Polyhedron* **1992**, *11*, 1075.

(13) Selected data for **2a**: IR (CH_2Cl_2) $\nu(\text{CO})$ 2077 s, 2044 s, 2004 s, 1988 m, 1964 w cm^{-1} ; $^{31}\text{P}\{^1\text{H}\}$ NMR (CDCl_3) δ 73.4 ppm; $^{13}\text{C}\{^1\text{H}\}$ NMR (CD_2Cl_2) δ 179.7 (d, $^2J_{\text{PC}} = 38.8$ Hz, CO), 179.0 (d, $^2J_{\text{PC}} = 28.7$ Hz, CO), 177.2 (d, $^2J_{\text{PC}} = 7.5$ Hz, CO), 176.1 (d, $^2J_{\text{PC}} = 5.0$ Hz, CO), 175.8 (d, $^2J_{\text{PC}} = 7.5$ Hz, CO), 174.9 (d, $^2J_{\text{PC}} = 5.0$ Hz, CO), 143.8 (d, $^2J_{\text{PC}} = 7.0$ Hz, C_{ipso}), 142.1 (s, C_α), 138.1 (d, $^1J_{\text{PC}} = 38.8$ Hz, C_{ipso}), 135.4–127.3 (mult, C_{phenyl}), 88.3 (s, C_β), -3.3 (s, C_γ) ppm; ^1H NMR (CD_2Cl_2) δ 7.7–6.8 (mult, 15H, H_{phenyl}), 2.54 (d, $^2J_{\text{HH}} = 6.2$ Hz, 1H, $=\text{CH}_a\text{H}_b$), 1.71 (dd, $^2J_{\text{HH}} = 6.2$ Hz, $^3J_{\text{PH}} = 2.5$ Hz, 1H, $=\text{CH}_a\text{H}_b$) ppm. Anal. Calcd for $\text{C}_{27}\text{H}_{17}\text{O}_6\text{POs}_2\text{CH}_2\text{Cl}_2$: C, 36.02; H, 2.05. Found: C, 36.23; H, 2.07.

(14) Although we favor this assignment on the basis of a comparison with the metallacycles **3** and **4** and 2-D $^{13}\text{C}\text{--}^1\text{H}$ spectra, the alternative assignment $\delta(\text{C}_\alpha)$ (**1a**, 99.2 ppm; **2a**, 88.3 ppm), $\delta(\text{C}_\beta)$ (**1a**, 141.1 ppm; **2a**, 142.1 ppm), $\delta(\text{C}_\gamma)$ (**1a**, 1.0 ppm; **2a**, -3.3 ppm) with C_β at lowest field is also possible. INADEQUATE ^{13}C NMR experiments failed to distinguish between these possibilities.

(15) Crystal data for **1a**: pale yellow 14-faced polyhedra from the slow evaporation of a $\text{CH}_2\text{Cl}_2/\text{C}_6\text{H}_{14}$ solution at 295 K, $\text{C}_{27}\text{H}_{17}\text{O}_6\text{PRu}_2\text{CH}_2\text{Cl}_2$, $M_r = 755.4$, tetragonal, space group $P4_32_12$, $a = 12.300(2)$ Å, $c = 37.671(7)$ Å, $Z = 8$, $V = 5699(2)$ Å³, $d_{\text{calc}} = 1.761$ g cm^{-3} , $\mu(\text{Mo K}\alpha) = 13.44$ cm^{-1} , $F(000) = 2976$. The structure was solved (Patterson/Fourier methods) and refined (full-matrix least squares) on the basis of 4305 observed ($F > 6.0\sigma(F)$) reflections measured at 175 K using Mo K α ($\lambda = 0.71073$ Å) radiation via the ω scan technique ($2\theta_{\text{max}} = 60.0^\circ$) on an LT-2-equipped Siemens R3m/V diffractometer. The final R and R_w values were 2.07 and 2.22%, respectively. The absolute structure was established using the unmerged (7393 observed) data and refining both possible enantiomorphs. This yielded final R and R_w values of 2.26 and 2.39% in the space group $P4_32_12$ and 2.56 and 2.72% in the space group $P4_12_12$, thus confirming the correct assignment.

(16) Crystal data for **2a**: pale yellow 14-faced polyhedra from the slow evaporation of a CH_2Cl_2 solution at 295 K, $\text{C}_{27}\text{H}_{17}\text{O}_6\text{POs}_2\text{CH}_2\text{Cl}_2$, $M_r = 933.7$, tetragonal, space group $P4_12_12$, $a = 12.285(1)$ Å, $c = 37.528(7)$ Å, $Z = 8$, $V = 5664(2)$ Å³, $d_{\text{calc}} = 2.190$ g cm^{-3} , $\mu(\text{Mo K}\alpha) = 92.5$ cm^{-1} , $F(000) = 3488$. The structure was solved and refined as for **1a** on the basis of 4237 observed ($F > 6.0\sigma(F)$) reflections measured at 175 K. The final R and R_w values were 4.18 and 4.43%, respectively. The absolute structure was established using the unmerged (7466 observed) data and refining both possible enantiomorphs. This yielded final R and R_w values of 5.98 and 6.93% in the space group $P4_32_12$ and 4.79 and 5.16% in the space group $P4_12_12$, thus confirming the correct assignment.

(17) (a) Schuchart, C. E.; Young, G. H.; Wojcicki, A.; Calligaris, M.; Nardin, G. *Organometallics* **1990**, *9*, 2417. (b) Schuchart, C. E.; Wojcicki, A.; Calligaris, M.; Faleschini, P.; Nardin, G. *Organometallics* **1994**, *13*, 1999.

(18) (a) Mealli, C.; Proserpio, D. M. *J. Chem. Educ.* **1990**, *67*, 399. (b) Hoffmann, R.; Lipscomb, W. N. *J. Chem. Phys.* **1962**, *36*, 2179, 3489. (c) Hoffmann, R. *J. Chem. Phys.* **1963**, *39*, 1397.

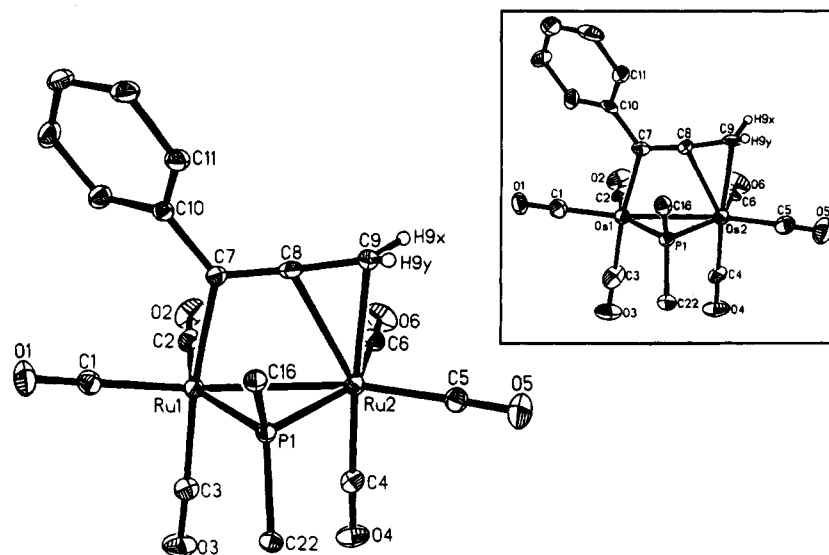
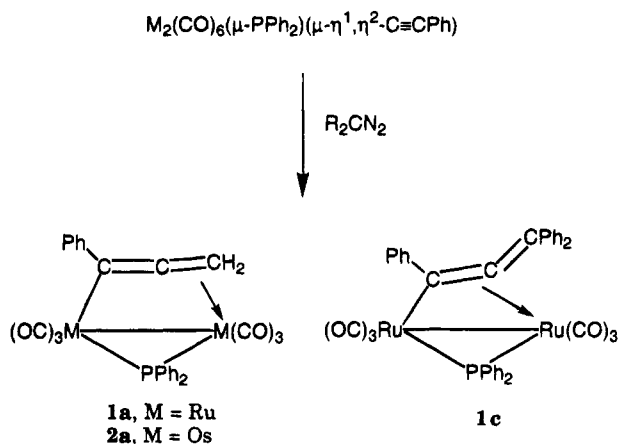


Figure 1. Molecular structure of $\text{Ru}_2(\text{CO})_6(\mu\text{-PPH}_2)(\mu\text{-}\eta^1\text{:}\eta^2_{\beta,\gamma}\text{-C(Ph)=C=CH}_2)$ (**1a**) illustrating the coordination mode of the allenyl ligand to the second metal site. For clarity, only the *ipso* carbon atoms of the phosphido bridge are shown. A view of the osmium analogue **2a** is shown in the insert.

Scheme 1



Despite extensive orbital mixing owing to the low symmetry of the molecule, the LUMO and SLUMO clearly have major contributions from the β -carbon, while C_α and C_γ make virtually no contribution. Thus, the observed regioselectivity of nucleophilic attack at C_β would appear to be under both charge and orbital control. As the allenyl group slips parallel to the $\text{M}(1)\text{-M}(2)$ bond toward $\text{M}(2)$ such that the $\text{M}(2)\text{-M}(1)\text{-C}(7)$ angle increases, the contribution from C_β to the LUMO increases, suggesting that the transition state may be close to the slipped geometry. Our EHMO studies also indicate that there is an essentially flat energy surface ($\Delta(\text{energy}) \approx 1 \text{ eV}$) on going from the bonding arrangement observed for **1a** to that observed for **1c**, with the former bonding mode slightly favored. The slightly less stable geometry results principally from a distortion of the $\text{Ru}_2(\text{CO})_6(\text{PH}_2)$ fragment on going from **1a** to **1c**. Indeed, if the geometry of the Ru_2P core is held constant and the bonding mode of the allenyl ligand shifts from $\mu\text{-}\eta^1\text{:}\eta^2_{\beta,\gamma}$ to $\mu\text{-}\eta^1\text{:}\eta^2_{\alpha,\beta}$, the two structural isomers are essentially isoenergetic.

Although the chemistry of **1a** with monodentate nucleophiles is dominated by nucleophilic attack at C_β , we have recently discovered that reactions with bidentate phosphines lead to a new reaction pathway. Reac-

tion (toluene, 60°C) of **1a** (0.230 g, 0.343 mmol) and DPPM (0.196 g, 0.510 mmol) results in the rapid, and high-yield (>60%) formation of $\text{Ru}_2(\text{CO})_4(\mu\text{-DPPM})[\mu\text{-}\eta^2\text{:}\eta^3\text{-P(Ph}_2\text{)C(O)C(Ph)CCH}_2]$ (**6**). Spectroscopic investigations¹⁹ suggested substantial rearrangement of both the supporting phosphido bridge and the C_3 hydrocarbyl fragment. The $^{31}\text{P}\{^1\text{H}\}$ NMR spectrum revealed three coupled resonances (δ 58.7 (dd, $^2J_{\text{PP}} = 240 \text{ Hz}$, 3 or $^4J_{\text{PP}} = 5 \text{ Hz}$, P_1), 44.1 (dd, $^2J_{\text{PP}} = 72 \text{ Hz}$, 3 or $^4J_{\text{PP}} = 5 \text{ Hz}$, P_3), 30.6 (dd, $^2J_{\text{PP}} = 240 \text{ Hz}$, 3 or $^4J_{\text{PP}} = 72 \text{ Hz}$, P_2) ppm) all at high field with respect to the shift of the phosphido bridge in **1a**. In the $^{13}\text{C}\{^1\text{H}\}$ NMR the diagnostic high-field shift assignable to C_γ of the hydrocarbyl ligand in **1a** (δ 1.0 ppm) was no longer observed. A single-crystal X-ray study provided full structural details²⁰ (Figure 2). The DPPM ligand has displaced two carbonyl ligands and adopts its familiar role of bridging two metal centers. The most remarkable feature of the structure, however, is the transformation of the allenyl ligand into a (formally) ketone-functionalized allene which is coupled to the phosphorus atom of the phosphido bridge, converting the latter into a phosphine. This coupling sequence results from a dual insertion of a carbonyl ligand into the Ru-C_α bond of the C_3 hydrocarbyl and into one arm of the phosphido bridge (Scheme 2). The synthesized ketoallenyl phosphine is a six-electron donor to the dimetal center. The near-linear arrangement of $\text{P}(1)\text{-Ru}(1)\text{-P}(2)$ ($177.0(1)^\circ$) accounts for the large (240 Hz) coupling observed in the $^{31}\text{P}\{^1\text{H}\}$ NMR spectrum. The C-C distances in the original C_3 ligand are significantly elongated in **6** ($\text{C}(6)\text{-C}(7) = 1.494(19)$

(19) Selected data for **6**: IR (CH_2Cl_2) $\nu(\text{CO})$ 2006 sh, 1991 vs, 1979 sh, 1949 s cm^{-1} ; $^{31}\text{P}\{^1\text{H}\}$ NMR (CDCl_3) δ 58.7 (dd, $^2J_{\text{PP}} = 240 \text{ Hz}$, $^4J_{\text{PP}} = 5 \text{ Hz}$, P_1), 44.1 (dd, $^2J_{\text{PP}} = 72 \text{ Hz}$, 3 or $^4J_{\text{PP}} = 5 \text{ Hz}$, P_3), 30.6 (dd, $^2J_{\text{PP}} = 240 \text{ Hz}$, 3 or $^4J_{\text{PP}} = 72 \text{ Hz}$, P_2) ppm; $^{13}\text{C}\{^1\text{H}\}$ NMR (CD_2Cl_2) δ 205.6 (d, $^2J_{\text{PC}} = 10.1 \text{ Hz}$, CO), 204.9 (t, $^2J_{\text{PC}} \approx 2J_{\text{PC}} = 10.6 \text{ Hz}$, CO), 197.0 (br q, $J_{\text{PC}} \approx 10.6 \text{ Hz}$, C=O), 178.6 (mult, C_β), 141.7–126.2 (mult, C_{phenyl}), 97.9 (dd, $^2J_{\text{PC}} = 76.5 \text{ Hz}$, $^2J_{\text{PC}} = 17.7 \text{ Hz}$, C_α), 71.7 (d, $^2J_{\text{PC}} = 19.9 \text{ Hz}$, C_γ), 50.8 (t, $^2J_{\text{PC}} \approx 2J_{\text{PC}} = 21.9 \text{ Hz}$, $-\text{CH}_2-$) ppm.

(20) Crystal data for **6**: yellow polyhedra from a concentrated CH_2Cl_2 solution at 263 K, $\text{C}_{51}\text{H}_{39}\text{O}_5\text{P}_3\text{Ru}_2\cdot 2\text{CH}_2\text{Cl}_2$, $M_r = 1196.7$, monoclinic, space group $\text{P}2_1/n$, $a = 15.190(5) \text{ \AA}$, $b = 23.550(6) \text{ \AA}$, $c = 15.281(4) \text{ \AA}$, $\beta = 108.02^\circ$, $Z = 4$, $V = 5198(2) \text{ \AA}^3$, $d_{\text{calc}} = 1.529 \text{ g cm}^{-3}$, $\mu(\text{Mo K}\alpha) = 9.25 \text{ cm}^{-1}$, $F(000) = 2408$. The structure was solved and refined as for **1a** on the basis of 5492 observed ($F > 6.0\sigma(F)$) reflections measured at 295 K. The final R and R_w values were 4.01 and 4.04%, respectively.

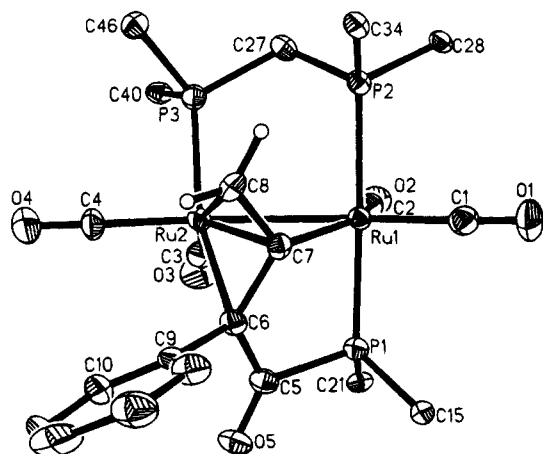
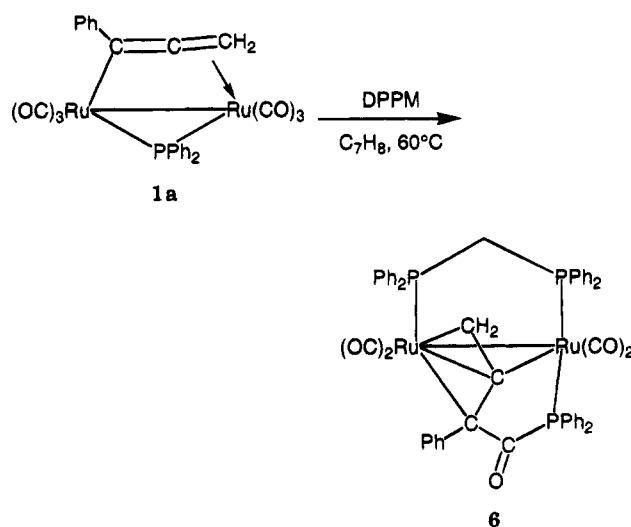


Figure 2. Perspective view of the molecular structure of $\text{Ru}_2(\text{CO})_4(\mu\text{-DPPM})[\mu\text{-}\eta^1\text{:}\eta^1\text{:}\eta^3\text{-P}(\text{Ph}_2)\text{C}(\text{O})\text{C}(\text{Ph})\text{CCH}_2]$ (**6**) illustrating the interaction of the ketoallenyl phosphine ligand to the two metal centers. For clarity, only the *ipso* carbon atoms of the phenyl rings on the phosphorus atoms are shown.

\AA ; $\text{C}(7)\text{-C}(8) = 1.421(15) \text{\AA}$) with a small angle at $\text{C}(7)$ ($\text{C}(6)\text{-C}(7)\text{-C}(8) = 111(1)^\circ$). The $\text{Ru}\text{-C}$ distances ($\text{Ru}(1)\text{-C}(7) = 2.148(11) \text{\AA}$; $\text{Ru}(2)\text{-C}(6) = 2.286(13) \text{\AA}$; $\text{Ru}(2)\text{-C}(7) = 2.120(11) \text{\AA}$; $\text{Ru}(2)\text{-C}(8) = 2.311(11) \text{\AA}$) indicate two short and two longer contacts. There is no precedent for coupling of allenyl, carbonyl, and phosphido groups to generate ketoallenyl phosphine ligands. However heterobimetallic allenylcarbonyls have recently been described,^{10,17} and the coupling sequence described here for allenyl complexes bears a resemblance to the chemistry observed for a heterobimetallic phosphido-alkyne complex.²¹

These results define a new coordination mode for the allenyl ligand and demonstrate the capability of the $\text{-C}(\text{R})=\text{C}=\text{C}\text{R}'\text{R}''$ fragment to use either one or both sets of orthogonal π orbitals for bonding in binuclear systems. This versatility and evidence that the allenyl

Scheme 2



groups can participate in new ligand coupling/insertion reactions point to a diverse chemistry for the cumulated ligand.

Acknowledgment. We are grateful to the Natural Sciences and Engineering Research Council of Canada for financial support of this work. N.C. was an exchange student at Waterloo from the University of Sussex. We also thank Prof. A. Wojcicki (Ohio State University) for the communication of his results prior to publication.

Supplementary Material Available: For **1a**, **2a**, and **6**, details of the structure determination (Tables S1, S7, and S13), non-hydrogen atomic positional parameters (Tables S2, S8, and S14), bond distances (Tables S3, S9, and S15), bond angles (Tables S4, S10, and S16), anisotropic thermal parameters (Tables S5, S11, and S17), and hydrogen atom positions (Tables S6, S12, and S18) (27 pages). Ordering information is given on any current masthead page. Observed and calculated structure factor tables are available from the authors upon request.

(21) Regragui, R.; Dixneuf, P. H.; Taylor, N. J.; Carty, A. J. *Organometallics* **1984**, *3*, 814.